Journal of Solid State Chemistry **143,** 62–68 (1999)
Article ID jssc.1998.8079, available online at http://www.idealibrary.com on IDEAL®

The Phase Diagram $CaO–Al_2O_3–Ta_2O_5$ and the Crystal Structures of Ca_2AlTaO_6 and $CaAlTaO_5$

M. Sales,* G. Eguia,† P. Quintana,‡ L. M. Torres-Martinez,† and A. R. West*

*Department of Chemistry, University of Aberdeen, Meston Walk, Aberdeen AB24 3UE, Scotland; †Facultad de Ciencias Quimicas, Universidad Autonoma de Nuevo Leon, Apartado Postal 1864, Monterrey, Nuevo Leon Mexico; and, ‡CINVESTAV IPN-Unidad Merida, Km. 6 Carretera antigua a Progreso, Cordemex, C.P. 97130,Merida, Yucatan, Mexico

Received August 3, 1998; in revised form October 15, 1998; accepted October 16, 1998

The subsolidus phase diagram $CaO–Al_2O_3–Ta_2O_5$ has been determined at 1300–1350°C. Two ternary phases are present, Ca_2AlTaO_6 and the new phase, $CaAlTaO_5$. From Rietveld refinement of powder X-ray diffraction data, $CaAlTaO_5$ has the sphene structure, monoclinic 6.6760(3), 8.9546(3), 7.3494(3) Å, $\beta = 114.098$ (3)°, space group $C2/c$, and Ca_2AlTaO_6 has a partially ordered double perovskite structure, monoclinic 5.3915(3), 5.4321(4), 7.6508(4) Å, $\beta = 90.076(5)°$, space group $P2_1/c$. The Al and Ta cations form a rock-salt-type arrangement with 3% cross substitution of Al on Ta sites and vice versa.

INTRODUCTION

Few studies on compound formation in the $CaO–Al_2O_3–Ta_2O_5$ system have been reported. No phase diagram is available and most work has focused on the phase Ca_2AlTaO_6, which is reported to be an ordered perovskite with $GdFeO_3$ structure and monoclinic symmetry (1). This phase was considered as a possible dielectric substrate for high-T_c superconductor films (2); it melts congruently at 1835°C and was suggested, instead, to have orthorhombic symmetry. The microwave dielectric properties of Ca_2AlTaO_6 ceramics (3) and $Ca_2AlTaO_6–CaTiO_3$ solid solutions (4) have been studied.

The three limiting two-component systems $CaO–Al_2O_3$, $CaO–Ta_2O_5$, and $Al_2O_3–Ta_2O_5$ are all well-established and contain a number of binary phases. Phase diagrams are available for $CaO–Al_2O_3$ (5) and $CaO–Ta_2O_5$ (6). For $Al_2O_3–Ta_2O_5$, only the binary phase $AlTaO_4$ is known (7).

In this study, we report a subsolidus phase diagram for the system $CaO–Al_2O_3–Ta_2O_5$ and crystal structure data for Ca_2AlTaO_6 and the new phase, $CaAlTaO_5$.

EXPERIMENTAL

Samples were prepared by solid state reaction of $CaCO_3$, Ta_2O_5, and Al_2O_3 (> 99%). The dried reagents were mixed in stoichiometric amounts and heated in Pt crucibles at 900–1350°C for a total of 2 to 30 days until either single phase products were obtained or no further reaction occurred. The heating conditions required to achieve equilibrium were determined by trial and error; once a particular reaction had apparently reached completion, the temperature was raised for an additional heating period. If no further reaction occurred, it was assumed that equilibrium had been reached.

Products were characterized by powder X-ray diffraction (XRD), using a Siemens D-5000 diffractometer. Diffraction data for indexing and refinement of the new phases were recorded using a Stoe STADI P diffractometer, Cu $K\alpha_1$ radiation, with the usual conditions of step scanning over an angular range $8° \leq 2\theta \leq 113°$ in increments of 0.02° (2θ) and with a counting time of 5 s for each step. Chemical composition of ternary phases was determined by a Cameca SX-51 EPMA on sintered and polished samples.

RESULTS AND DISCUSSION

Phase Formation and the $CaO–Al_2O_3–Ta_2O_5$ Phase Diagram

As a result of heating mixtures with different compositions over a range of temperatures and times, the conditions needed to obtain complete reaction and to form the equilibrium phase(s) were obtained. In general, a final firing at 1300–1350 °C for 2–3 days was sufficient to complete reaction. Some samples were heated as high as 1450°C, and no change in phase assemblage was observed.

It soon became apparent that, in addition to the various binary phases, two ternary phases were formed. From powder XRD analyses of the reaction products (Table 1) and EPMA analyses on selected compositions (Table 2), the subsolidus phase diagram was established and, at the same time, the compositions of the two ternary phases were determined, as Ca_2AlTaO_6 and $CaAlTaO_5$. Samples of

0022-4596/99 $30.00

TABLE 1
Crystalline Products of Heating Some Selected Compositions

$CaO:Al_2O_3:Ta_2O_5$ molar ratio	Temperature (°C)	Time (days)	Crystalline phases
71.5:20.0:8.5	1350	2	C4AT + C4T + C3A
71.5:7.0:21.5	1380	1	C4AT + C4T + C2T
66.7:26.5:6.8	1330	1	C4AT +C3A +C12A7
66.7:13.3:20.0	1350	2	C4AT + C2T
66.7:6.7:26.6	1450	2	C4AT + C2T
60.0:35.0:5.0	1350	1	C4AT + C12A7 + CA
60.0:10.0:30.0	1400	1	C2AT + C2T + α-CT_t
56.5:20.0:23.5	1400	1	C4AT + C2AT + C2T
56.0:7.0:37.0	1400	1	C2AT + C2T + α-CT
55.0:40.0:5.0	1350	3	C4AT + CA
55.0:22.5:22.5	1275	30	C4AT + C2AT
50.0:45.0:5.0	1350	2	C4AT + CA + CA2
50.0:35.0:15.0	1400	1	C4AT +C2AT +CA6
50.0:25.0:25.0	1275	13	C2AT + $C2T_t$
40.0:40.0:20.0	1275	30	C2AT + A_t + β-CT_t
40.0:30.0:30.0	1275	13	C2AT + β-CT + A_t
35.0:60.0:5.0	1350	2	C4AT + CA2 + CA6
30.0:35.0:35.0	1350	3	β-CT + CT2 + A
20.0:60.0:20.0	1400	1	β-CT + A
20.0:20.0:60.0	1350	2	CT2 + AT
15.0:80.0:5.0	1400	1	C2AT + CA6 + A
14.0:13.0:73.0	1350	2	CT2 + T + AT
10.0:50.0:40.0	1350	2	CT2 + AT + A

Note. C4AT, Ca_2AlTaO_6; C2AT, $CaAlTaO_5$; C4T, $Ca_4Ta_2O_9$; C2T, $Ca_2Ta_2O_7$; α-CT, α-$CaTa_2O_6$; β-CT, β-$CaTa_2O_6$; CT2, $CaTa_4O_{11}$; C3A, $Ca_3Al_2O_6$; C12A7, $Ca_{12}Al_{14}O_{33}$; CA, $CaAl_2O_4$; CA2, $CaAl_4O_7$; CA6, $CaAl_{12}O_{19}$; AT, $AlTaO_4$; A, Al_2O_3; T, Ta_2O_5; t, traces.

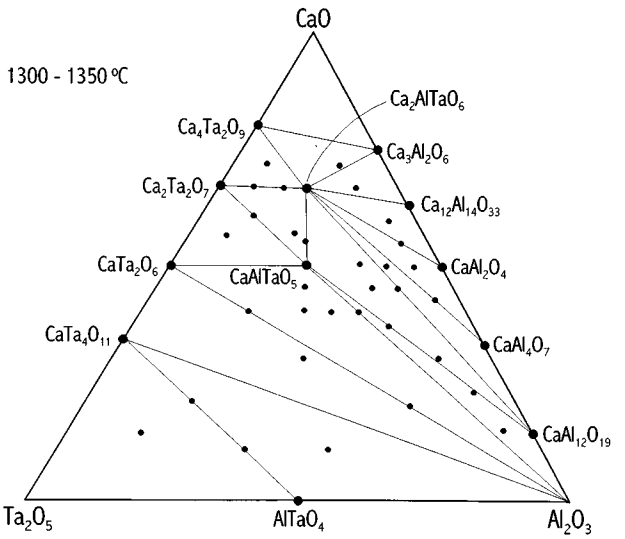

FIG. 1. Subsolidus phase diagram $CaO–Al_2O_3–Ta_2O_5$. Compositions studied are marked by solid circles: large circles represent single phase samples; small circles represent phase mixtures.

these compositions were single phase by XRD (lower limit of detection of secondary phases $\sim$2–3%) and by SEM/EPMA. The compositions determined by EPMA (Table 2) agreed with the expected compositions to within $\pm$ 1–3%. There was no evidence of solid solution formation and it is concluded, therefore, that these are stoichiometric phases.

TABLE 2
Composition of the Ternary Phases Determined by EPMA

Sample	Sintering treatment	Composition
Ca_2AlTaO_6	1450°C/101 h	$Ca_{1.972(5)}Al_{1.002(4)}Ta_{1.014(5)}O_{6.011(3)}$
$CaAlTaO_5$	1450°C/101 h	$Ca_{1.016(8)}Al_{1.002(6)}Ta_{1.032(4)}O_{5.011(3)}$

Note. Based on analysis of at least 10 different regions of the samples. Numbers in parentheses refer to the e.s.d.'s, which indicated an accuracy to the third decimal place.

The subsolidus phase diagram at 1300–1350°C is shown in Fig. 1; it is divided into 15 compatibility triangles, many of which contain either or both of the ternary phases, Ca_2AlTaO_6 and $CaAlTaO_5$, as constituents. For most regions of the diagram, melting temperatures are considerably in excess of 1350°C and have not been determined. Compositions in triangles containing $Ca_{12}Al_{14}O_{33}$ as one of the phases melt at around 1300°C, however. Although most of the results used to construct Fig. 1 were obtained at 1300–1350°C, we have no evidence or reason to believe that the diagram changes at higher, or lower, subsolidus temperatures.

Crystal Structure of $CaAlTaO_5$

The structure of $CaAlTaO_5$ was determined to be sphene-like from a combination of trial-and-error indexing of the powder XRD pattern and a literature search for related phases with similar cell dimensions. The unit cell is monoclinic; unit cell dimensions and indexed powder XRD data are given in Table 3; fully indexed powder XRD data for both phases have been deposited with the ICDD. Rietveld refinement was carried out using the atomic coordinates of $NaTaGeO_5$ (7) as starting parameters. Final coordinates are listed in Table 4, and a selection of bond lengths and angles are given in Table 5. An XRD profile and difference plot is shown in Fig. 2.

As in the parent sphene, $CaTiSiO_5$ (8), the structure consists of zigzag chains of corner-sharing TaO_6 octahedra parallel to *c* linked at their corners by AlO_4 tetrahedra to

TABLE 3
X-Ray Powder Diffraction Data

d_{obs} (Å)	I	hkl
(a) $CaAlTaO_5$; monoclinic $a = 6.6760(3)$ Å, $b = 8.9546(3)$ Å, $c = 7.3494(3)$ Å, $\beta = 114.098(3)^\circ$; space group $C2/c$ (15) $Z = 4$		
5.0412	100	110
4.4775	33	020
3.3647	85	$\bar{1}12$
3.0472	40	200
2.9280	4	$\bar{2}02$
2.6818	80	130
2.5188	11	220
2.4503	15	$\bar{2}22$
2.4372	18	112
2.3608	2	$\bar{1}13$
2.3477	4	131
2.3052	5	$\bar{1}32$
2.2377	7	040
2.1136	17	$\bar{3}12$
1.9809	12	310
1.9308	4	132
1.8616	12	042
1.8153	9	$\bar{2}04$
1.8037	6	240
1.7815	12	$\bar{1}14$
(b) Ca_2AlTaO_6; monoclinic $a = 5.3915(3)$ Å, $b = 5.4321(4)$ Å, $c = 7.6508(5)$ Å, $\beta = 90.076(5)^\circ$, space group $P2_1/n$ (14) $Z = 2$		
4.2469	62	011
4.4047	42	$\bar{1}01$, 101
3.8272	56	110
3.8228	53	002
3.4259	1	$\bar{1}11$, 111
2.7139	24	020
2.7043	100	112
2.6965	17	200
2.3126	17	$\bar{1}21$, 121
2.3087	27	013
2.3046	32	$\bar{1}03$, 103
2.3009	22	$\bar{2}11$, 211
2.0475	1	$\bar{1}22$, 122
2.0414	1	$\bar{2}12$, 212
1.9136	45	220
1.9112	30	004
1.8553	1	$\bar{2}21$, 221
1.7613	4	031
1.7575	13	$\bar{1}23$, 123
1.7540	8	$\bar{2}13$, 213
1.7480	8	$\bar{3}01$, 301
1.7160	5	130
1.7117	9	$\bar{2}22$, 222
1.7102	13	$\bar{1}14$, 114
1.6747	2	$\bar{1}31$, 131
1.5663	2	$\bar{1}32$, 132
1.5632	19	$\bar{2}04$, 204
1.5614	9	
1.5596	16	$\bar{3}12$
1.5578	22	312
1.4754	2	$\bar{2}31$, 231
1.4724	5	$\bar{1}05$, 105
1.4704	7	$\bar{3}21$, 321
1.3583	4	040
1.3531	10	$\bar{2}24$
1.3521	6	224
1.3482	4	400
1.2958	4	$\bar{2}33$
1.2941	5	233
1.2894	3	$\bar{4}11$, 411
1.2777	3	$\bar{1}34$, 134
1.2740	3	$\bar{3}14$
1.2725	4	314
1.2706	2	$\bar{4}02$, 402
1.2105	7	$\bar{3}32$
1.2097	8	332
1.2074	4	420

form a three-dimensional framework (Fig. 3). Ca occupies singly capped trigonal prisms which share common edges with AlO_4 tetrahedra and four TaO_6 octahedra. Hence, $CaAlTaO_5$ is structurally similar to $CaTiSiO_5$ and phases such as $NaTaGeO_5$. It does, however, represent a new cation charge combination for the sphene structure, i.e., II, III, V compared with II, IV, IV in sphene itself and I, IV, V in $NaTaGeO_5$. Bond lengths (Table 5) are consistent with those expected for coordination numbers of 7(Ca), 6(Ta), and 4(Al). Bond angles show that the TaO_6 octahedra and AlO_4 tetrahedra are almost undistorted. The high thermal parameter for Ca indicates the possibility of some positional disorder involving slight displacements from the positions given in Table 4.

TABLE 4
Atomic Parameters for $CaAlTaO_5$ (e.s.d. in Parentheses)

Atom	x	y	z	U_{iso} (Å^2)	Occupancy factor	Wyckoff site symmetry
Ca(1)	0	0.3355(7)	0.75	0.029(3)	1.00	4*e*
Al(1)	0	0.3163(11)	0.25	0.008(3)	1.00	4*e*
Ta(1)	0	0	0	0.0056(2)	1.00	4*e*
O(1)	0.1939(12)	0.4350(8)	0.4183(13)	0.002(1)	1.00	8*f*
O(2)	0.1058(13)	0.2038(9)	0.1132(13)	0.002(1)	1.00	8*f*
O(3)	0	0.0725(13)	0.75	0.005(2)	1.00	4*e*

Note. Number of reflections: 261. Number of parameters: 29 (15 structural parameters). *R*-factors: $R_p = 7.72\%$; $R_{wp} = 10.45\%$; $R_{exp} = 8.6\%$; $R_I = 5.51\%$.

Crystal Structure of Ca_2AlTaO_6

This phase was reported previously (1) and was suggested to be monoclinic with a perovskite-related structure but a full structure determination was not carried out. Its XRD pattern could not be indexed in the usual orthorhombic *Pbnm* space group for the $GdFeO_3$ structure type because of the presence of extra reflections; in addition, some of the peak intensities were very different from those of, e.g., Ca_2FeTaO_6 (9) which has the $GdFeO_3$ structure. The possibility of *B*-site order of Al and Ta was therefore considered. In the literature on related phases, two ordered structures are well established, with either a rock-salt-like or layered arrangement of the *B* cations. The rock salt ordered structures are either cubic, with $a = 2a_p$ and space group $Fm3m$ or monoclinic, with a unit cell $\sqrt{2}a_p$, $\sqrt{2}a_p$, $2a_p$ and space group $P2_1/c$. The layered structures are monoclinic with a unit cell $2a_p$, $2a_p$, $2a_p$ and space group $P2_1/m$ (10).

The powder XRD data for Ca_2AlTaO_6 could be fully indexed using a monoclinic, rock-salt-type cell (Table 3). A starting model used for the structure solution and refinement was that of Ca_2CrTaO_6 (11), which has a partially ordered $GdFeO_3$ structure with *B* cations in a rock-salt-like array. Refinement of this model with ordering of Al and Ta

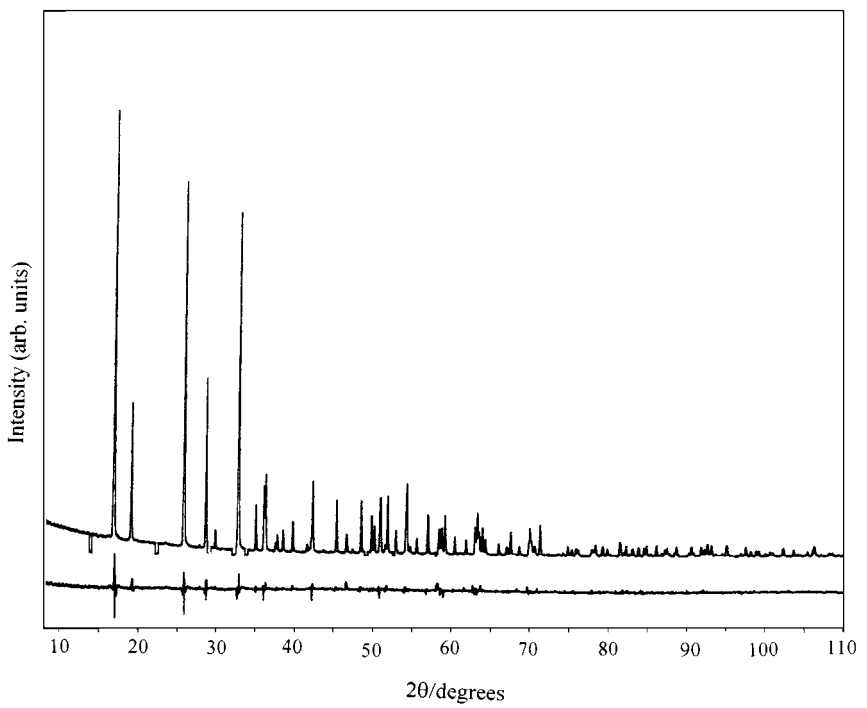

FIG. 2. Observed and difference XRD profile for $CaAlTaO_5$.

TABLE 5
Bond Distances (Å) and Bond Angles (°) for $CaAlTaO_5$

Distances			
Ca(1)–O(1)		2.470(9)	×2
O(2)		2.729(9)	×2
O(2)		2.425(9)	×2
O(3)		2.351(13)	
Average Ca(1)–O		*2.514(10)*	
Ta(1)–O(1)		1.965(9)	×2
O(2)		2.007(8)	×2
O(3)		1.945(4)	×2
Average Ta(1)–O		*1.972(7)*	
Al(1)–O(1)		1.737(10)	×2
O(2)		1.759(10)	×2
Average Al(1)–O		*1.748(10)*	
Angles			
O(1)–Ta(1)–O(2)	89.8(3) ×2	O(2)–Ta(1)–O(3)	92.7(3) ×2
O(1)–Ta(1)–O(2)	90.2(3) ×2	O(1)–Al(1)–O(1)	104.7(5)
O(1)–Ta(1)–O(3)	89.2(3) ×2	O(1)–Al(1)–O(2)	107.4(5) ×2
O(1)–Ta(1)–O(3)	90.8(3) ×2	O(1)–Al(1)–O(2)	113.5(5) ×2
O(2)–Ta(1)–O(2)	87.3(3) ×2	O(2)–Al(1)–O(2)	110.3(5)

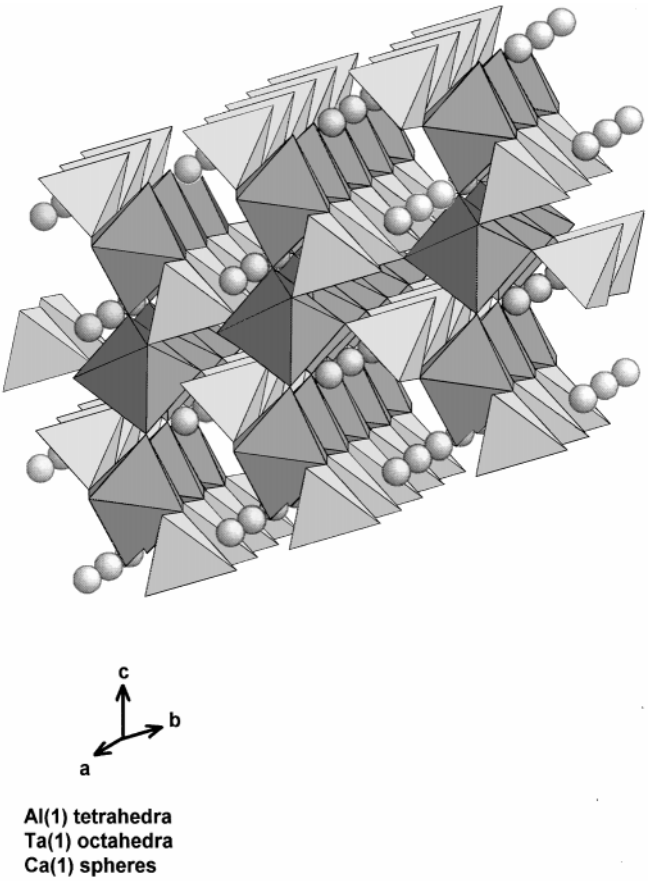

FIG. 3. Crystal structure of $CaAlTaO_5$ showing framework formed from TaO_6 octahedra and AlO_4 tetrahedra.

gave satisfactory atomic positions but a negative thermal parameter for Al. This indicated possible partial occupancy of the Al sites by Ta, and vice versa. Models with various partial occupancies were tested and their refinement parameters compared. The Al site was found to be particularly sensitive to the degree of Ta occupancy and the final model adopted contained 97(1) Al, 3(1) Ta for the Al site and *vice versa* for the Ta site. Final refined parameters, bond lengths, and angles are listed in Tables 6 and 7; XRD profiles are shown in Fig. 4 and a structural drawing is shown in Fig. 5.

The crystal structure is an example of the well-established $GdFeO_3$ structure with *B*-site order of cations in the rock-salt arrangement. Rietveld refinement indicated about 3% cross substitution between Al and Ta sites. Such partial cross substitution is found in several other related structures: Sr_2CrTaO_6 (0.66 to 0.34 occupancy ratios),

TABLE 6
Atomic Parameters for Ca_2AlTaO_6 (e.s.d. in Parentheses)

Atom	*x*	*y*	*z*	U_{iso} (Å^2)	Occupancy factor	Wyckoff site symmetry
Ca(1)	0.020(2)	0.0327(7)	0.7502(7)	0.0182(11)	1.00	4*e*
Al(1)	0	0.5	0	0.0123(11)	0.97	2*c*
Ta(1)	0	0.5	0	0.0123(11)	0.03	2*c*
Al(2)	0.5	0	0	0.0164(3)	0.03	2*d*
Ta(2)	0.5	0	0	0.0164(3)	0.97	2*d*
O(1)	0.270(3)	0.292(3)	0.973(4)	0.004(2)	1.00	4*e*
O(2)	0.305(3)	0.278(2)	0.551(4)	0.004(2)	1.00	4*e*
O(3)	0.923(3)	0.486(3)	0.744(2)	0.004(2)	1.00	4*e*

Note. Number of reflections: 276. Number of parameters: 31 (17 structural parameters). *R*-factors: $R_p = 6.37\%$; $R_{wp} = 8.60\%$; $R_{exp} = 5.7\%$; $R_I = 7.69\%$.

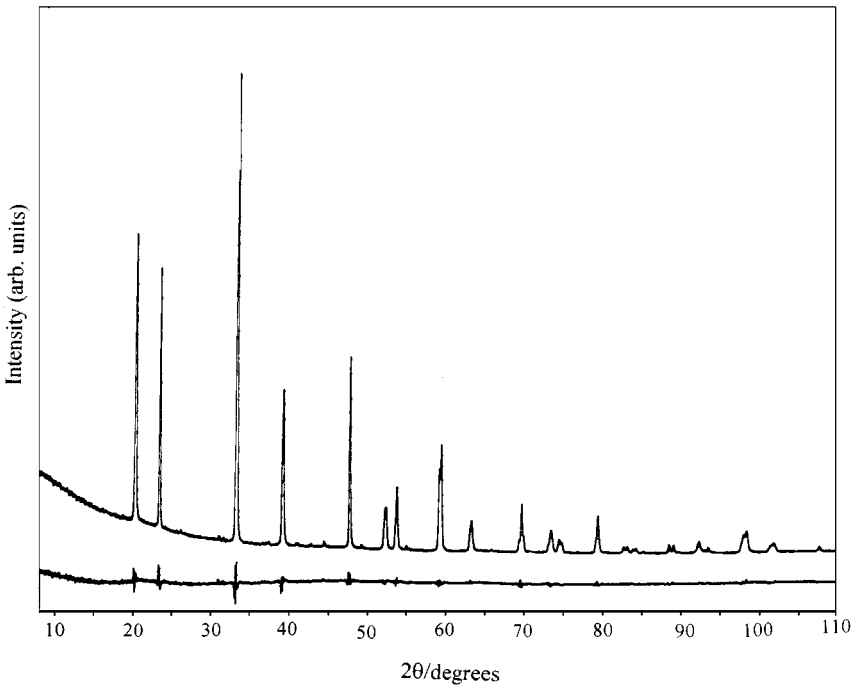

FIG. 4. Observed and difference XRD profile for Ca_2AlTaO_6.

Ca_2CrTaO_6 (0.73 to 0.27 occupancy ratios) (11), Sr_2FeSbO_6 (0.80 to 0.20 occupancy ratios) (12), and $SrLaNiSbO_6$ (0.90 to 0.10 occupancy ratios) (13).

The bond lengths (Table 7) show that the Al site is somewhat smaller than the Ta site, as expected from usual Al–O and Ta–O bond distances. The Ca site is a somewhat distorted, eight-coordinate site, again with a range of reasonable Ca–O bond distances.

TABLE 7
Bond Distances (Å) and Bond Angles (°) for Ca_2AlTaO_6

Distances					
Ca(1)–O(1)	2.43(2)		Ca(1)–O(2)	2.54(2)	
Ca(1)–O(1)	2.59(2)		Ca(1)–O(2)	2.77(3)	
Ca(1)–O(1)	2.68(3)		Ca(1)–O(3)	2.40(2)	
Ca(1)–O(2)	2.25(2)		Ca(1)–O(3)	2.51(1)	
Average Ca(1)–O			*2.52(2)*		
Al/Ta(1)–O(1)		1.85(2)		× 2	
O(2)		1.88(2)		× 2	
O(3)		2.00(1)		× 2	
Average Al/Ta(1)–O			*1.91(2)*		
Ta/Al(2)–O(1)		2.02(2)		× 2	
O(2)		2.07(2)		× 2	
O(3)		1.91(1)		× 2	
Average Ta/Al(2)–O			*2.00 (2)*		
Angles					
O(1)–Al/Ta(1)–O(2)	88.4(9) × 2		O(1)–Ta/Al(2)–O(2)	92.8(9) × 2	
O(1)–Al/Ta(1)–O(2)	91.6(9) × 2		O(1)–Ta/Al(2)–O(2)	87.2(9) × 2	
O(1)–Al/Ta(1)–O(3)	91.8(8) × 2		O(1)–Ta/Al(2)–O(3)	86.3(8) × 2	
O(1)–Al/Ta(1)–O(3)	88.2(8) × 2		O(1)–Ta/Al(2)–O(3)	93.7(8) × 2	
O(2)–Al/Ta(1)–O(3)	93.2(8) × 2		O(2)–Ta/Al(2)–O(3)	88.0(7) × 2	
O(2)–Al/Ta(1)–O(3)	86.8(8) × 2		O(2)–Ta/Al(2)–O(3)	92.0(7) × 2	

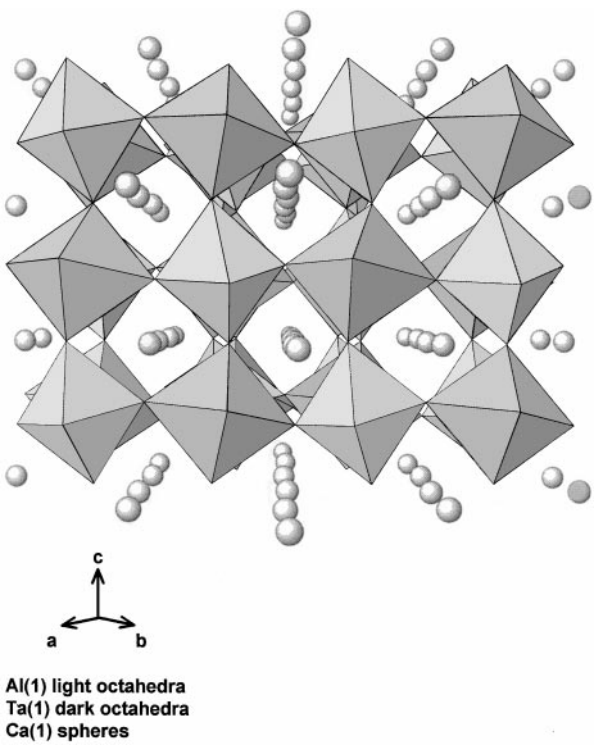

FIG. 5. Crystal structure of Ca_2AlTaO_6 showing framework of corner-sharing $(Ta_{0.97}Al_{0.03})O_6$ and $(Al_{0.97}Ta_{0.03})O_6$ octahedra.

ACKNOWLEDGMENTS

We thank Dr. A.M. Coats for assistance with the EPMA analysis. M.S. thanks the Ministerio de Educacion y Ciencia (Spain) for her grant. We thank CONACYT for financial support for the Catedra Patrimonial de Excelencia Nivel II (970030), to P.Q., and for financial support for Projects 3824P-A9607 and 3862P-A9607, to G.E. and L.M.T.M.

REFERENCES

1. V. S. Filip'ev and E. G. Fesenko, *Sov. Phys. Crystallogr.* **10,** 243 (1967).
2. C. D. Brandle and V. J. Fratello, *J. Mater. Res.* **5,** 2160 (1990).
3. H. Kagata and J. Kato, *Jpn. J. Appl. Phys.* **33,** 5463 (1994).
4. S. Kucheiko, J.-W. Choi, H.-J. Kim, and H.-J. Jung, *J. Am. Ceram. Soc.* **79,** 2739 (1996).
5. A. K. Chatterjee and G.I. Zhmoidin, *J. Mater. Sci.* **7,** 93 (1972).
6. D. A. Reeve, *J. Less-Common Metals* **17,** 218 (1969).
7. E. A. Gorkina and B.V. Mill, *Sov. Phys. Crystallogr.* **37,** 769 (1992).
8. C. R. Robbins, *Mat. Res. Bull.* **3,** 693 (1968).
9. J. A. Chavez, Ph.D. thesis, University of Aberdeen 1995.
10. M. T. Anderson, K. B. Greenwood, G. A. Taylor, and K. R. Poeppelmeier, *Prog. Solid State Chem.* **22,** 197 (1993).
11. J.-H. Choy, J.-H. Park, S.-T. Hong, and D.-K. Kim, *J. Solid State Chem.* **111,** 370 (1994).
12. E. J. Cussen, J. F. Vente, P. D. Battle, and T. C. Gibb, *J. Mater. Chem.* **7,** 459 (1997).
13. M. P. Attfield, P. D. Battle, S. K. Bollen, T. C. Gibb, and R. J. Whitehead, *J. Solid State Chem.* **100,** 37 (1992).